Materials Horizons

Sustainable Mechanochemical Growth of Double-Network Hydrogels Supported by Vascular-like Perfusion

Journal:	*Materials Horizons*
Manuscript ID	MH-COM-07-2023-001038.R1
Article Type:	Communication
Date Submitted by the Author:	02-Aug-2023
Complete List of Authors:	Wei, Gumi; Hokkaido University Graduate School of Life Science Kudo, Yumeko; Hokkaido University Graduate School of Life Science Matsuda, Takahiro; Hokkaido University Graduate School of Life Science Wang, Zhi Jian; Hokkaido University Institute for Chemical Reaction Design and Discovery, (WPI-ICReDD) Mu, Qi Feng; Hokkaido University Graduate School of Life Science King, Daniel; Hokkaido University Faculty of Advanced Life Science Nakajima, Tasuku; Hokkaido University Faculty of Advanced Life Science; Hokkaido University Institute for Chemical Reaction Design and Discovery, (WPI-ICReDD) Gong, Jian Ping; Hokkaido University Faculty of Advanced Life Science; Hokkaido University Institute for Chemical Reaction Design and Discovery, (WPI-ICReDD)

New concept

In this work, we developed a metabolic-like growth system that enabled a long-term mechanochemical growth of double-network (DN) hydrogels in air. We have found that DN hydrogels subjected to mechanical deformations can generate a high concentration of mechanoradicals owing to the sacrificial bond cleavage, and significantly consumed the preloaded monomers in the DN gel. To continuously deliver monomers for the mechanoradical polymerisation in DN gels, a channel-containing double-network hydrogel (c-DN gel) was fabricated. The c-DN gel can be connected to an external circulation system for a vascular-like perfusion through the inner channel. This system not only enabled a sustainable supply of monomers during mechanoradical polymerisations but also replenished the water loss and prevented drying of gels in the air. We demonstrated that the system can support the repetitive self-strengthening of DN gels that lasted for hours in deoxygenated air. The metabolic-like growth of c-DN gels in response to cyclic loading exhibited similarities to the strengthening and hypertrophy of muscles supported by the vascular circulation.

COMMUNICATION

Sustainable Mechanochemical Growth of Double-Network Hydrogels Supported by Vascular-like Perfusion

Received 00th January 20xx,
Accepted 00th January 20xx

DOI: 10.1039/x0xx00000x

Gumi Wei,[a] Yumeko Kudo,[a] Takahiro Matsuda,[a] Zhi Jian Wang,[b] Qi Feng Mu,[a] Daniel R. King,[†c] Tasuku Nakajima,*[bc] and Jian Ping Gong*[bc]

Double-network (DN) gels are unique mechanochemical materials owing to their structures that can be dynamically remodelled during use. The mechanical energy applied to DN gels is efficiently transferred to the chemical bonds of the brittle network, generating mechanoradicals that initiate the polymerisation of pre-loaded monomers, thereby remodelling the materials. To attain continuous remodelling or growth in response to repetitive mechanical stimuli, a sustainable supply of chemical reagents to such dynamic materials is essential. In this study, inspired by the vascular perfusion transporting nutrients to cells, we constructed a circulatory system for a continuous supply of chemicals to channel-containing DN hydrogels (c-DN gels). The perfusion of monomer solutions through the channel and permeability of the c-DN gels not only replenishes the monomers consumed by the polymerisation but also replenishes the water loss caused by the surface evaporation of hydrogel, thereby freeing the mechanochemical process of DN gels from the constraints of the underwater environment. The facile chemical supply enabled us to modulate the mechanical enhancement of the c-DN gel and attain muscle-like strengthening under repeated mechanical training in deoxygenated air. We also studied the kinetics of polymer growth and strengthening and deciphered unique features of mechanochemical reaction in DN gels including the extremely long-living radicals and delayed mechanical strengthening.

Introduction

Muscle building is a mechanochemical process in which mechanical work is used to trigger chemical reactions for muscle hypertrophy. Mechanical training intensity and frequency influence the extent of damage to muscle fibres, while nutrients such as amino acids and minerals chemically affect tissue reconstruction.[1] Muscle growth provides a fascinating model for material innovations. However, a few examples are available that demonstrate the construction of artificial muscles that are able to grow and remodel themselves based on the transformation of mechanical work into chemical reactions.[2] Recently, we proposed a mechanochemical strategy for hydrogel growth by using double-network (DN) hydrogels.[3] A DN hydrogel is made from two interpenetrated networks with contrasting properties; one is hard and brittle, and the other is soft and stretchable. Owing to these contrasting properties, the chemical bonds of the brittle network are highly susceptible to macroscopic mechanical stimuli.[4] The mechanical energy applied to a DN material causes chemical bond scissions in the brittle network, which generate large amounts of mechanoradicals or introduce mechanophores, thereby imparting new functions such as thermal sensitivity[5], self-strengthening,[3, 6] force stamp-induced surface patterning,[7] and damage mapping[5, 8, 9] to the DN gel.

To achieve sustainable remodelling or growth of DN gels in response to repeated mechanical stimuli, replenishing the monomers consumed during polymerisation is essential. In previous studies, the DN hydrogels were immersed in monomer solutions during the mechanochemical process to replenish the monomers, which significantly limited their usage. In the current study, inspired by vascular perfusion,[10-12] we constructed a circulatory system that enabled a sustainable supply of monomers to channel-containing DN hydrogels. This self-sustainable system can simultaneously control the circulation of the monomer solutions and mechanical deformation. Using this system, we successfully achieved the continuous muscle-like hypertrophy of DN gels in deoxygenated air. We also used this system to investigate the kinetics of mechanochemical growth in DN gels. With the continuous circulation of the monomers, an extended polymerisation time (~1 h) was observed using Raman spectroscopy. We discuss this

[a] Graduate School of Life Science, Hokkaido University, Sapporo 001-0021, Japan.
[b] Institute for Chemical Reaction Design and Discovery (WPI-ICReDD), Hokkaido University, Sapporo 001-0021, Japan.
[c] Faculty of Advanced Life Science, Hokkaido University, Sapporo 001-0021, Japan.
E-mail: tasuku@sci.hokudai.ac.jp; gong@sci.hokudai.ac.jp.
† The author passed away on May 1, 2022.
Electronic Supplementary Information (ESI) available: See DOI: 10.1039/x0xx00000x

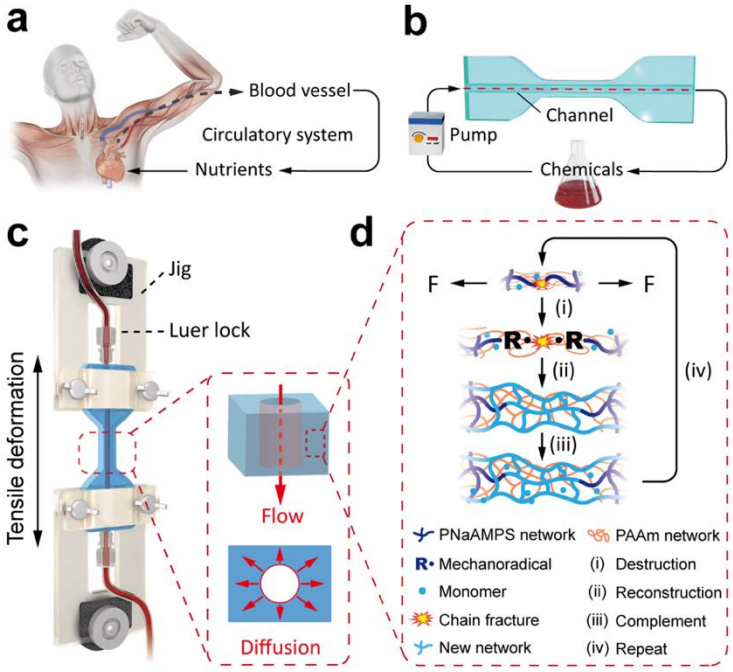

Fig. 1 Bioinspired design of sustainable mechanochemical growth of hydrogel with vascular-like perfusion. (a) Illustration of muscle growth by mechanical training. The vascular circulation supplies the nutrients for the growth.[‡] (b) Illustration of a channel-containing double network hydrogel (c-DN gel) connected to a circulatory bath of monomer solution for muscle-like mechanochemical growth. (c) Illustration of the metabolic-like system to show a repetitive self-growth of c-DN hydrogel under mechanical training. With the circulation system, a continuous supply of monomers through diffusion from the channel is attained. (d) Mechanism of the muscle-like growth of c-DN hydrogel: stretching of the c-DN gel triggers internal fracturing of the rigid network (dark blue), generating chain-end radicals and initiating the polymerisation of monomers to form a new network (light blue). With continuous flow through the channel to sustain the mechanoradical polymerisations, the system enables the c-DN gel to grow continuously under repetitive stretching.

unique polymerisation behaviour from the viewpoint of the possible long lifetimes of mechanoradicals tethered to a polymer network.

Results and discussion

Construction of the c-DN gel and circulatory system

Muscle growth is supported by the vascular system, through which nutrients are sustainably supplied via heart-driven blood circulation (Fig. 1a). Similarly, we designed a circulation system for sustainable mechanochemical growth of DN hydrogels (Fig. 1b). The system consisted of a channel-containing double network hydrogel (c-DN gel), chemical solution reservoir, and pump, all of which were connected by soft and flexible tubes. The chemicals (monomers) were supplied through a tube by pumping the solution from the reservoir into the c-DN gels. The chemicals diffused into the gel matrix through the channel wall because of the intrinsic permeability of the hydrogels (Fig. 1c)[13]. Under mechanical stretching, the mechanoradicals produced in the c-DN hydrogel by the rupture of the brittle network efficiently initiated polymerisation of the diffused monomers, reconstructing the structure of the c-DN gel (Fig. 1d). Mechanoradical polymerisation consumed chemicals in the gel, which induced additional diffusion of chemicals from the channel into the gel. Consequently, mechanoradical polymerisation occurred continuously within the lifetime of the mechanoradicals. Therefore, the c-DN gel was expected to exhibit self-strengthening under cyclic mechanical loading. Similar to muscle training, which is influenced by the workout plan and nutrient supply,[14] the self-strengthening of c-DN gels also relies on the chemical supply and force triggers. This system can independently control the chemical supply and mechanical loading simultaneously, enabling us to probe the details of the force-triggered mechanoradical polymerisation in c-DN gels.

We used DN gels with poly(2-acrylamido-2-methylpropanesulfonic acid) sodium salt (PNaAMPS) as the first network and poly(acrylamide) (PAAm) as the second network. This DN gel was prepared in a formulation that produces ~10^{-5} M mechanoradicals at a strain of 7 (Experimental section, Fig. S1). The internal channel of the DN hydrogel was fabricated using sacrificial moulds (Experimental section and Fig. S2, S3). Photographs of the c-DN gel are shown in Fig. 2a. A channel with a diameter of ~1.6 mm was located at the centre of the gauge and evenly crossed through the sample from one side to the other. To connect the channel of the c-DN gel to the circulation system, the two ends of the channel were connected to flexible tubes using Luer locks (Fig. 2b). Owing to the elastic and tough properties of the c-DN gel, no liquid leakage occurred when the c-DN gel was subjected to deformations, such as stretching or bending (Fig. 2b, movie S1). To place the c-DN gel in the tensile machine, the two clamping regions were fixed using specially designed jigs (Fig. S4). This setup enabled liquids to flow in the channel during cyclic tensile loading (Fig. 2c). Thus, the channel in the c-DN hydrogel functioned perfectly as a liquid-delivery pathway during tensile tests.

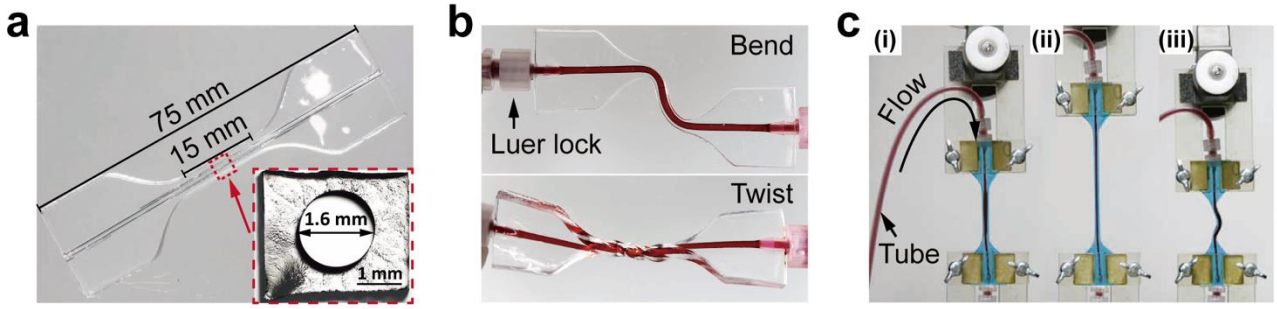

Fig. 2 (a) Photograph of the fabricated c-DN gel in dumbbell shape for cyclic tensile loading. The insert photo shows the cross-sectional photo of the gel in gauge region, as indicated by an arrow. (b) Photos of the c-DN gel under bending and twisting without leakage of the flowing liquid (dyed in red). (c) Photos of c-DN gel (dyed in blue) during tensile test.

As a permeable substance, the c-DN hydrogel allowed the diffusion of chemicals from the channel into the gel matrix, which was visually confirmed by the circulating liquid containing brilliant green molecules (Fig. S5). According to the Stokes-Einstein equation,[15-17] the diffusion coefficient D for a monomer of typical size R ~1 nm is of the order of D ~10^{-10} m^2/s in aqueous media at room temperature. Thus, the characteristic time for a monomer to diffuse from the channel wall to the edge of the gauge (l = 1 mm) was approximately estimated as $t = l^2/D$ ~10^4 s. To confirm this, we detected monomer diffusion into the c-DN gels using attenuated total reflection Fourier transform infrared (ATR-FTIR) spectroscopy (Fig. S6). ATR-FTIR signals were collected from the outer surface of the c-DN gel, and the time profile of the monomer concentration was obtained using a calibration curve. The diffusion of the two monomers used in the subsequent experiments, *N*-isopropylacrylamide (NIPAAm) and 2-acrylamido-2-methyl-1-propanesulfonic acid sodium salt (NaAMPS), was measured. The liquid circulation speed was set at 0.13 mL/s. For NIPAAm, the symmetrical deformation vibration absorption peaks of the isopropyl group located at 1371 and 1388 cm^{-1} were monitored (Fig. S7).[18] With the circulation of a 1 M NIPAAm aqueous solution, the NIPAAm concentration at the outer surface gradually increased with time and eventually saturated in 90 min.

A similar saturation time (~90 minutes) was observed with the circulation of 0.1 M NaAMPS, where the signal of the characteristic asymmetric stretching of sulfonic group peak ($\nu_{S=O}$) of NaAMPS at 1043 cm^{-1} was monitored[19-21] (Fig. S8). These results show that the two monomers diffused into the DN gels and reached an equilibrium concentration at ~90 min, independent of their concentration in the circulating solution. The observed results are consistent with the diffusion theory. In addition, the perfusion of aqueous solutions through the channel can replenish the water loss and prevent drying, which solves the problem of hydrogels in the air due to the surface evaporation of water.[22] This is demonstrated by the long-term cyclic tensile tests of the c-DN gel in the air at room temperature (Fig. S9). Without water circulation, the c-DN gel gradually dehydrated and became brittle, and eventually fractured within 2 h, whereas the gel with water circulation remained moist and soft, even after 12 h of cyclic tensile testing, indicating that the c-DN gel maintained a stable water content. Hence, vascular-like perfusion not only replenishes chemicals but also water, which paves the way for continuous self-strengthening in a dry environment through hours of cyclic mechanical training.

Diffusion-limited mechanoradical polymerisation

Subsequently, mechanoradical polymerisation profiles of the stretched c-DN gels were observed. The experiments were performed in an Ar-purged glovebox under a deoxygenated atmosphere. For visualizing polymerisation, we adopted NIPAAm as the monomer, following a previous work.[5] As illustrated in Fig. 3a, the mechanoradicals generated by the deformation of c-DN gel initiated NIPAAm polymerisation, forming temperature-responsive poly(*N*-isopropylacrylamide) (PNIPAAm) in the c-DN gel. By elevating the temperature above the lowest critical solution temperature (LCST) of PNIPAAm (~32 °C), the newly formed PNIPAAm became hydrophobic and underwent a coil-globule transition, which can be visualised by the 8-anilino-1-naphthalene sulfonic acid (ANS) that fluoresces in hydrophobic environments.[23, 24]

Because the diffusion of the monomer from the channel wall to the entire cross-sectional area requires 90 min, which is much longer than the time required for mechanical deformation (a loading–unloading cycle typically took 1–2 min in this study) and radical polymerisation (typically less than a minute)[7], we can visualise the monomer diffusion process based on the aforementioned strategy by performing a preflow test (Fig. 3b). Particularly, after circulating the NIPAAm aqueous solution (1 M) in the c-DN hydrogel for various durations (2, 5, 10, 15, 30, 60, and 90 min), the circulation was stopped, and a tensile stretch to a displacement of 105 mm (a strain of 7) was applied to the sample at a velocity of 300 mm/min, triggering the mechanoradical polymerisation of NIPAAm in the gel. After the tensile stretch was released, the sample was immediately exposed to open air to quench the polymerisation, and the gauge part was sliced into 1 mm-thick slices and immersed in ANS aqueous solution for laser scanning confocal microscopy (LSCM).

As shown in Fig. 3c, green fluorescence was observed in all the stretched samples after perfusion with the NIPAAm aqueous solution, indicating the formation of PNIPAAm by in situ mechanoradical polymerisation. The fluorescent area developed from the channel wall towards the outer surface with increasing circulation time and eventually reached a spatially uniform distribution in 90 min.

Because the mechanical damage to the gel by tensile deformation was almost uniform in the sample, the

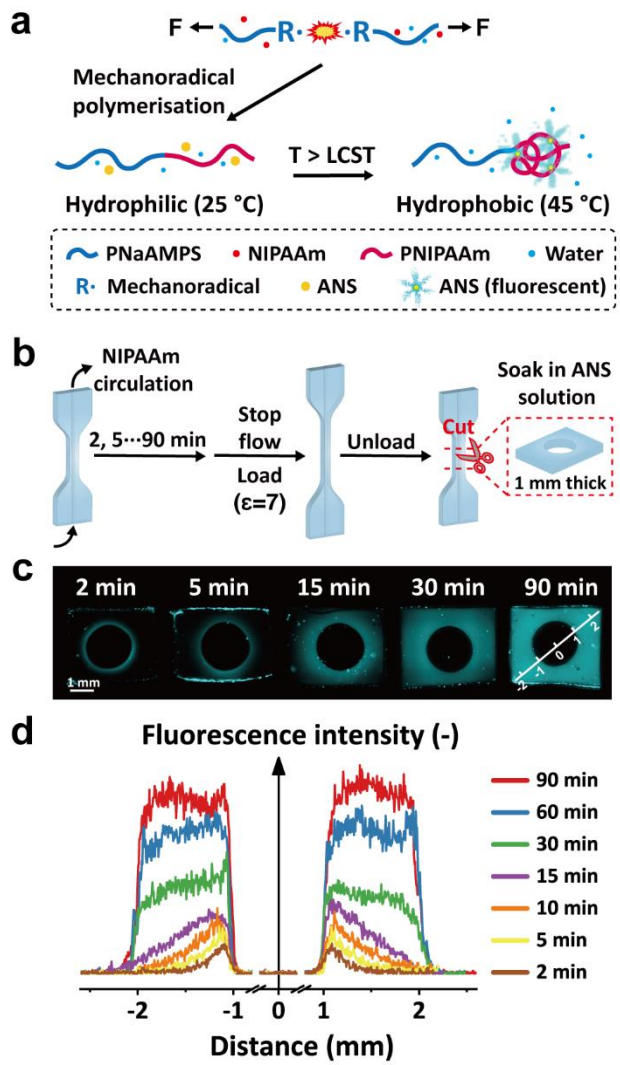

Fig. 3 Visualization of the diffusion of the monomer molecules by fluorescence distribution. (a) Fluorescence mechanism of the prestretched DN hydrogel fed by NIPAAm, the mechanoradicals generated by the breaking of the first network initiate in-situ polymerisation of NIPAAm supplied from the internal circulatory flow, and form PNIPAAm chains (red). The thermoresponsive PNIPAAm is detected by fluorescent ANS. Only the broken chain in the DN gel is shown. (b) Illustration of the protocol to prepare the preflow samples, a tensile stretch of 300 mm/min to a strain of 7 (with the upper jig raising to 105 mm) is applied after a preset circulation time. (c) Fluorescent images of the preflow cross-sectional slices, the white scale bar arranged in a diagonal direction on the 90-min sample indicates the position to measure the line profiles of fluorescence intensity in 'd'. (d) Fluorescence intensity line profiles of the cross-sectional slices of the preflow samples with various flow times.

fluorescence distribution corresponded to the concentration distribution of NIPAAm at different circulation times. Fig. 3d shows the fluorescence intensity distributions along the diagonal direction (as indicated by the white line in the 90 min sample in Fig. 3c) for different durations of circulation. An intensity gradient from the centre to the outer surface was observed even when the diffusion time was only 2 min, owing to the high monomer concentration gradient at the beginning of circulation. After 90 min of circulation, the fluorescence intensity finally became homogeneous, which agreed with the ATR-IR results (Fig. S7 and S8) and corresponds to the diffusion equilibrium. While in situ reactions in polymer matrices are drawing more attention from researchers[12, 25], these results verify that the c-DN gel can be adopted as a long-term mechanoradical system working in a dry environment.

Muscle-like cyclic strengthening sustained by continuous flow

After the successful mechanoradical polymerisation of NIPAAm in the c-DN gel, cyclic tensile tests were performed to achieve mechano-induced c-DN gel strengthening while perfusing the c-DN gel with a continuous flow. To achieve self-strengthening, an elastically effective network needs to be formed in the sample via mechanoradical polymerisation. Therefore, an aqueous solution containing NaAMPS as a monomer and *N,N'*-methylenebisacrylamide (MBAA) as a crosslinker was circulated during the cyclic tensile test. The samples were coded as M_aC_b, where a and b are the molar concentrations of the monomer (M) and cross-linker (C), respectively, in the flow solution. For example, the $M_{0.10}C_{0.10}$ sample indicates a flow solution containing 0.10 M NaAMPS and 0.10 M MBAA. Before the cyclic tensile test, the sample was circulated for 1.5 h to allow the reactants in the c-DN gel to reach equilibrium. After each loading–unloading cycle, a resting time of 1 h was set before the next cycle. Subsequent experiments demonstrated that, by 1 h, a new network triggered by the mechanoradicals generated in the previous cycle could be formed.

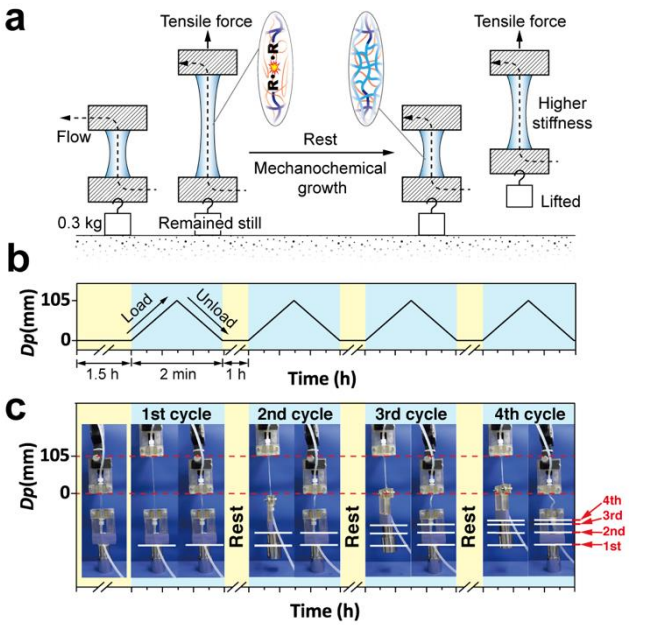

Fig. 4 Muscle-like behaviours of the c-DN hydrogel under repeated mechanical deformations. (a) Illustration of the training process of the c-DN hydrogel by mechanochemical growth. The upper jig is fixed to the tensile tester and repeatedly lifted up to a displacement of 105 mm, the lower jig is connected to a weight (0.3 kg). After the "training" sustained independently by the vascular perfusion, the c-DN hydrogel is able to lift up the weight. (b) Protocol of the upper crosshead displacement during the cyclic deformation of the c-DN gel (gauge length = 15 mm). (c) Demonstrations of the muscle-like behaviours of a c-DN hydrogel supplied by 0.10 M NaAMPS monomer and 0.10 M MBAA crosslinker ($M_{0.10}C_{0.10}$) showing repetitive stretch-triggered mechanical growth.

First, cyclic tensile tests were performed using a fixed tensile force. Therefore, the lower end of the c-DN gel was connected to a weight. A 0.3 kg weight was used to induce the yielding of the virgin c-DN gel (Fig. 4a). The upper jig was moved cyclically following the protocol shown in Fig. 4b. Fig. 4c shows the images of the muscle-like strengthening behaviour of $M_{0.10}C_{0.10}$. The corresponding video is shown in Movie S2. As indicated by the line marking the locations of the weight attached to the lower jig, although the weight remained still in the first cycle, it was raised to higher locations in successive loadings, resembling muscles that became stronger and lifted weights during strength training. The difference in the weight-lifted height between each cycle gradually decreased, indicating that the c-DN gel became stiffer with the cyclic lifting.

Subsequently, cyclic tensile tests were conducted under a fixed tensile strain. In this test, the lower jig was kept stationary, and the upper jig was moved upward for a displacement *of Dp* = 105 mm, at which point the gel reached complete necking and then returned to the neutral position (*Dp* = 0) of the virgin gel (Fig. 5a). As a typical example, the force profile of the $M_{0.10}C_{0.10}$ sample in response to cyclic tensile deformation is shown in Fig. 5b. The response of the $M_{0.00}C_{0.00}$ sample (perfused with pure water) is shown for comparison.

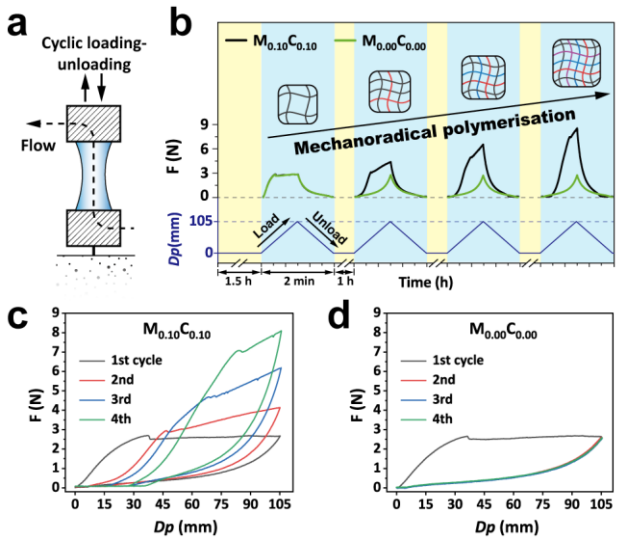

Fig. 5 Stretch-triggered repetitive self-growth of c-DN gel by continuous monomer supply from the internal channel. (a) Illustrator of the cyclic loading–unloading setup. (b) Force–time curves of $M_{0.10}C_{0.10}$ under a repeated tensile force trigger shown in the loading–unloading protocol underneath: the upper crosshead displacement (*Dp*) is lifted up to 105 mm and then returned to the original position (*Dp* = 0 mm) during the cyclic deformation of the c-DN gel (gauge length = 15 mm). The gel shows an noticeable strengthening due to repeated network deconstruction–reconstruction. $M_{0.00}C_{0.00}$ implies the flow of pure water as a reference, which indicates no self-growth without monomers supply from the channel. Samples are coded by the concentrations of monomer and cross-linker in the flowing solution as M_aC_b, where "a" stands for the monomer (NaAMPS) concentration and "b" the cross-linker (MBAA) concentration (all in mol/L). (c, d) Force–displacement curves of the $M_{0.10}C_{0.10}$ (c), and $M_{0.00}C_{0.00}$ (d) samples, respectively, under four times of repeated tensile force trigger as shown in the lower panel in 'b'.

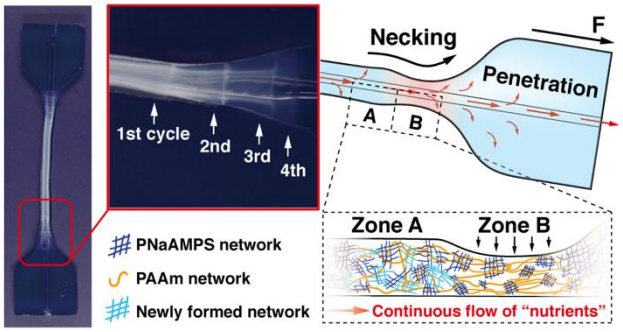

Fig. 6 Appearance of $M_{0.10}C_{0.10}$ sample after four times of self-growth and the illustration of the unevenly distributed structure which caused the whitening phenomenon. As the gauge region yielded by stretch, it became stiffer by self-strengthening. Therefore, the relatively "weaker part" outside the yielded zone starts to yield in the next stretch. Thus, translucent "scars" of "training" that distinctly indicates the occurrence of four times of self-strengthening were left.

The $M_{0.10}C_{0.10}$ sample showed successive strengthening with cyclic loading, as evidenced by the force curve surpassing the previous curve, whereas the $M_{0.00}C_{0.00}$ sample (perfused with pure water) showed no strengthening. By combining the force–time profiles and displacement–time protocol in Fig. 5b, we obtained the force–displacement curves of the $M_{0.10}C_{0.10}$ and $M_{0.00}C_{0.00}$ samples for four cycles, as depicted in Fig. 5c and d, respectively. The critical displacement to show the force gradually increased with the number of cycles owing to an increase in the gauge length by growth, whereas that of the $M_{0.00}C_{0.00}$ sample hardly changed. What is more, combined with the cross-sectional size of self-grown samples (Fig. S10), we can draw the conclusion that the strength and size of the samples both increased by remodelling the structure under cyclic mechanical training. We observed four translucent "scars" outside the gauge region, which distinctly indicate the occurrence of four times of self-strengthening (Fig. 6). As the gauge region yielded by stretching, it became stiffer owing to self-strengthening. Therefore, the relatively "weaker part" outside the yielded part started to yield in the next stretch cycle to show the training scars.

The strengthening effect in the solution strongly depended on the concentrations of the monomer and cross-linker in the solution (Fig. 7a and Fig. S11, 12). The M_aC_b samples can be classified into three groups: no growth, slight growth, and remarkable growth, depending on the flowing monomer and crosslinker concentrations (Fig. 7b). Sample $M_{0.08}C_{0.0}$ with no crosslinker exhibited no strengthening, similar to $M_{0.00}C_{0.00}$, confirming that the newly formed polymer must be crosslinked for strengthening. Samples of $M_{0.02}C_{0.02}$ and $M_{0.00}C_{0.04}$ showed slight growth, indicating that only a sparse network was formed at low monomer and crosslinker concentrations. Samples of a = b ≥ 0.04 M showed remarkable growth and successive strengthening was observed with the cyclic tensile loading.

To quantify the extent of self-growth, the yield force (F_y), stiffness, and hysteresis were measured, as shown in Fig. 7c.

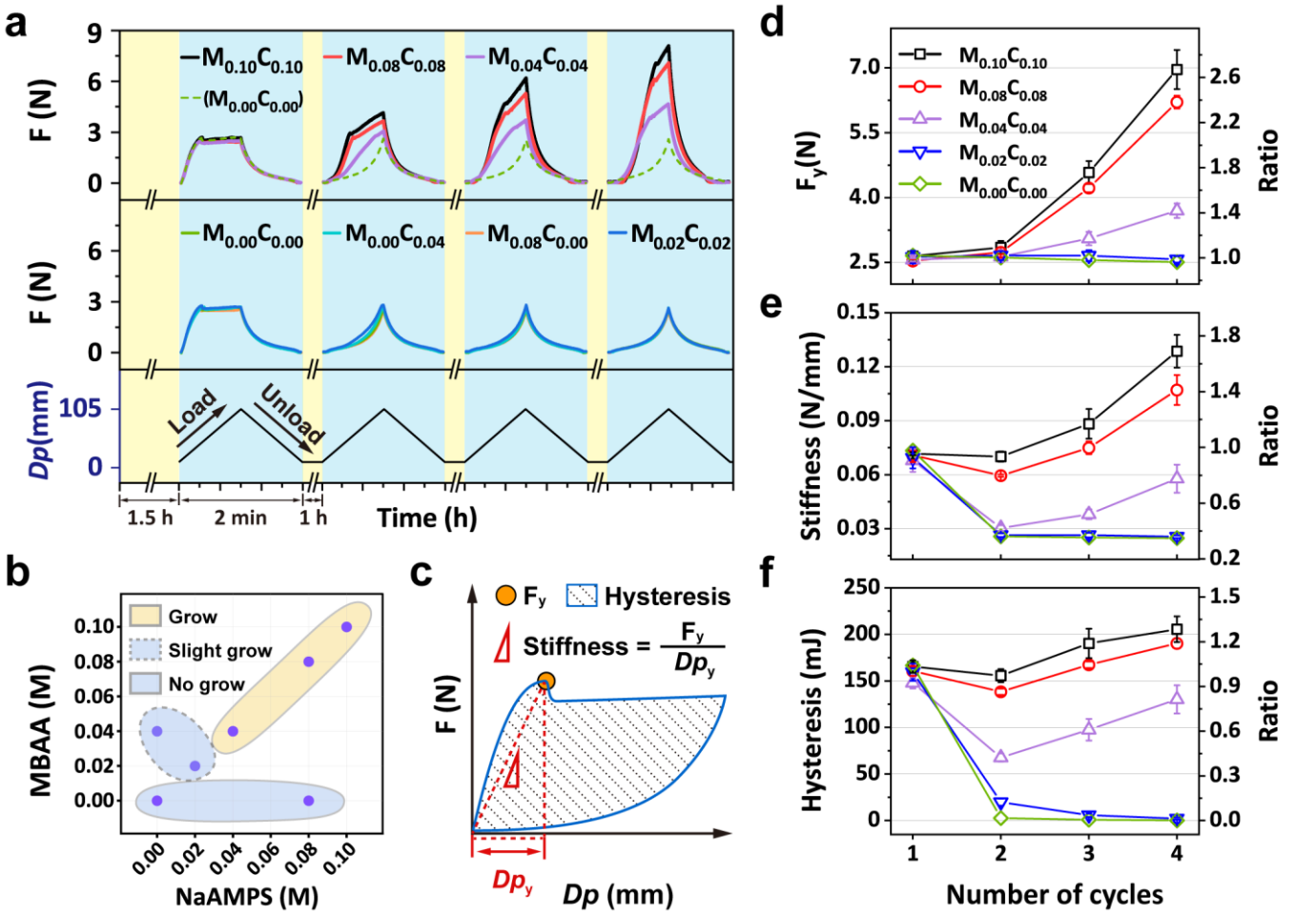

Fig. 7 Effect of monomer and cross-linker concentration supplied through the channel on self-strengthening. (a) Result of force enhancement of various samples as a function of time, the loading–unloading process is conducted as the protocol in the lower panel, groups shown in the upper panel ($M_{0.10}C_{0.10}$, $M_{0.08}C_{0.08}$, $M_{0.04}C_{0.04}$) exhibit noticeable self-growth ($M_{0.00}C_{0.00}$ implies the flow of pure water as a blank control group), while the middle panel ($M_{0.00}C_{0.00}$, $M_{0.00}C_{0.04}$, $M_{0.08}C_{0.00}$, $M_{0.02}C_{0.02}$) exhibits only slight or no self-growth. (b) Group summary according to the reactant supply and self-growth result. (c) Definition of mechanical parameters for evaluating the extent of self-growth from the loading–unloading curve of a cyclic tensile test. (d–f) Variations and the ratio of change that are relative to the original value of mechanical parameters during four times of self-growth: d. yield force (F_y); e. stiffness; and f. hysteresis.

The parameters summarised from the force–displacement curves are compared in Fig. 7d–f. For the $M_{0.10}C_{0.10}$, $M_{0.08}C_{0.08}$, and $M_{0.04}C_{0.04}$ samples, F_y, stiffness, and hysteresis all showed increasing trends from the second to the fourth cycle. It is also worth noticing that for an effective repeated self-growth, the amount of cross-linker should be comparable to the monomer in the fed solution. Otherwise, as shown in Fig. S13, the $M_{0.25}C_{0.10}$ sample with a higher a/b ratio fractured in the 2nd stretch owing to an excess swelling introduced by the newly formed polyelectrolyte network with more NaAMPS units. The PAAm network, by swelling-induced dilution, became too weak to bear the load transferred from the broken rigid network, resulting the sample failure.[26]

Because a higher yield force and stiffness correspond to a denser network, the increasing trend indicates that a denser network was newly formed after each cycle. The hysteresis loop area, which indicates the energy dissipated in the polymer network fracturing at each cycle, increases with the number of cycles. These results indicate that successive structural reconstruction occurs at the expense of the deconstruction of the network formed in the previous cycle. The decrease in stiffness after the first loading, especially for the M_aC_b samples with a = b < 0.08 is owing to the partial fracture of highly prestretched strands of the initial first network by fracture. The strands in the newly formed network are in a relaxed state and should exhibit lower stiffness than the pre-stretched strands.[27, 28] Nevertheless, the F_y, stiffness, and hysteresis increased with the number of tensile cycles and surpassed those in the first cycle. This indicates that the newly formed network is denser than the first network in the virgin sample.

In summary, mechanoradical polymerisation in the presence of a sufficient amount of monomer and crosslinker (a = b ≥ 0.04 M) resulted in an elastically effective new network. This newly formed densely crosslinked network not only enhanced the mechanical performance of the c-DN hydrogel but also sacrificed itself to generate mechanoradicals upon force triggers. Therefore, the c-DN gel underwent repetitive mechanochemical growth and exhibited muscle-like self-strengthening during the subsequent cycles.

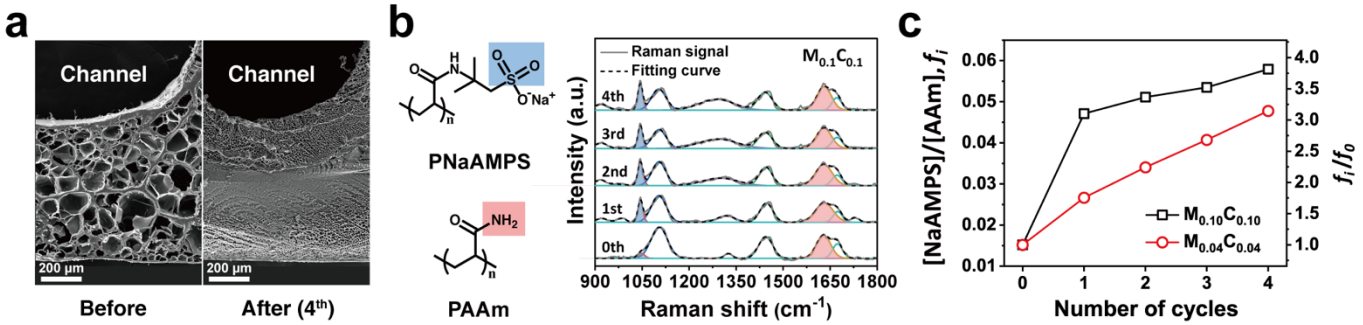

Fig. 8 Quantitative determination of the amount of polymerised PNaAMPS with repetitive mechanical training. (a) Cross-sectional SEM images of the c-DN gel ($M_{0.10}C_{0.10}$) before, and after the fourth cycle of tensile force-triggered mechanoradical polymerisation (scale bar: 200 μm). (b) Raman spectroscopy of $M_{0.10}C_{0.10}$ samples during four times of stretch, the fitted peak at 1045 cm^{-1} corresponds to the S=O stretching in PNaAMPS (marked as blue), and the peak at 1630 cm^{-1} corresponds to the NH_2 scissoring in PAAm (marked as red). (c) Molar ratio of the NaAMPS units to AAm units in the hydrogel matrix as a function of the number of cycles.

Polymer mass increase with cyclic training

The newly formed polymer network increases the polymer density of the c-DN gel. We observed an increase in the polymer mass of the c-DN gel during self-growth. Fig. 8a shows scanning electron microscopy (SEM) images of the freeze-dried $M_{0.10}C_{0.10}$ sample before and after four cycles, as described in the previous section. Notably, while the virgin sample exhibited a typical honeycomb-like morphology owing to the evaporation of water, the porous appearance was hardly observed after four training cycles. The latter indicates an increase in the polymer content by mechanoradical polymerisation.

The increase in polymer content was then quantitatively analysed using Raman spectroscopy, which allowed the study of the changes in the chemical composition of the hydrogel. Here, we collected the Raman spectra of the $M_{0.10}C_{0.10}$ (Fig. 8b) and $M_{0.04}C_{0.04}$ samples in their new equilibrium state after self-growth(Fig. S14, Table S1), and Gaussian fitting was used to analyse the relative content changes caused by the mechanochemical growth. The band intensity at 1045 cm^{-1}, corresponding to the S=O stretching of NaAMPS units[20], increased gradually with more tensile cycles, which is a direct chemical proof of the newly formed PNaAMPS network by the mechanochemical process.[29] The peak at 1630 cm^{-1}, corresponding to the NH_2 scissoring vibrations of the PAAm second network,[30, 31] remained constant during mechanoradical polymerisation, as expected. By measuring the ratio R of the absolute areas of the peaks at 1045 cm^{-1} (marked in blue) and 1630 cm^{-1} (marked in red), we estimated the molar ratio f of the NaAMPS units relative to AAm units in the c-DN gel using the following equation:

$$f_i = f_0(R_i/R_0), \quad (1)$$

where f_i and f_0 are the molar ratios of NaAMPS units to AAm units in the i^{th} and 0^{th} (virgin c-DN gel) cycles, respectively, and R_i and R_0 are the area ratios of the peak at 1045 cm^{-1} to that at 1630 cm^{-1} in the i^{th} and 0^{th} cycles, respectively. The initial molar ratio f_0 (0.015) was calculated from the reagents added during c-DN gel fabrication, neglecting the small-quantity components of the crosslinker and initiator. Fig. 8c shows the molar ratio f as a function of the mechanical training cycles for the $M_{0.04}C_{0.04}$ and $M_{0.10}C_{0.10}$ samples. Although the $M_{0.04}C_{0.04}$ sample showed a remarkable decrease in stiffness after the first cycle, as shown in Fig. 7, polymer growth was clearly observed after the first cycle and increased with cyclic mechanical training. Moreover, the amount of polymer growth in $M_{0.10}C_{0.10}$ was larger than that in $M_{0.04}C_{0.04}$. This is consistent with the more efficient mechanical training of the $M_{0.10}C_{0.10}$ sample observed in Fig. 7.

Kinetics of mechanochemical growth and delayed strengthening

Similar to the strengthening and hypertrophy of muscles, the self-growth of DN gels requires time for mechanochemical reactions. In this study, the kinetics of mechanochemical growth and strengthening were investigated. As shown by the protocol in Fig. 9a, we applied the first stretch cycle to trigger mechanoradical generation in the gels and then allowed the gels to rest for a preset time varying from 5 to 360 min to allow new network formation in the gels. Subsequently, we applied a second stretch cycle to measure the mechanical enhancement of the gels by growth during the rest time. During the entire process, the c-DN gels were continuously circulated with the aqueous solution containing 0.1 M NaAMPS monomer and 0.1 M MBAA crosslinker ($M_{0.10}C_{0.10}$).

Fig. 9b shows the force–displacement curves of the first and second stretching cycles. The stiffness and hysteresis as a function of the resting time were extracted from the curves of the second cycle, as shown in Fig. 9e. These results clearly show that the gels achieved remarkable strengthening in ~1 h, and then gradually reached a constant state, although the monomers were continuously supplied to the gels by circulation throughout the entire process.

The growth of the PNaAMPS at different resting times was further detected by Raman spectroscopy, and the results are shown in Fig. 9c and Fig. S15. The peak signal from PNaAMPS at 1045 cm^{-1} increased with resting time up to 360 min. The molar ratios f of NaAMPS units relative to the AAm units at various time was calculated from the corresponding area ratio of the peak at 1045 cm^{-1} to that at 1630 cm^{-1} (Fig. S15), as shown in Fig. 9d. We observed that PNaAMPS had more than double its original molar ratio within 5 min, more than half of the total newly formed PNaAMPS for a growth time of 360 min.

Compared with Fig. 9e, we noticed that the hysteresis and stiffness only exhibited a mild increase in the first 5 min. This delayed strengthening compared to polymer growth is further highlighted in the plots of stiffness and hysteresis as a function

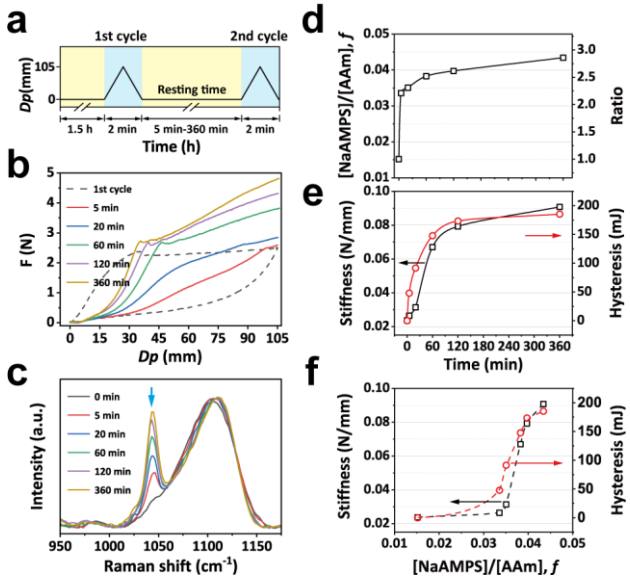

Fig. 9 Kinetic process of self-strengthening by mechanochemical growth. (a) Protocol of the two cyclic stretch cycles. A resting time for growth was set between the first and the second cycles. During the whole process, the c-DN gels were continuously circulated with the monomer solution (0.1 M NaAMPS, 0.1 M MBAA). (b) Force–displacement curve of the c-DN gels for the first cycle and loading curves of the second cycle after various resting time. (c) Raman spectra of c-DN gels for various resting times, the peak at 1045 cm^{-1} pointed by a blue arrow corresponds to the signal of *v* (S=O) originated from the growing PNaAMPS during the resting time. (d, e) Growth-time dependencies of chemical and mechanical parameters: d. Unit mole ratio of NaAMPS to AAm (*f*); e. stiffness (left axis) and hysteresis (right axis). (f) Correlations between the molar ratio of NaAMPS/AAm and stiffness (left axis) and hysteresis (right axis). The dashed line is a visual guide.

of the molar ratio *f* in Fig. 9f. The results show that the newly formed PNaAMPS can only strengthen the gels above a critical content (*f* = 0.03), which is twice that of the virgin DN gels (*f* = 0.015). Such a discrepancy in the kinetics of polymer growth and mechanical strengthening can be attributed to the delayed cross-linking reaction compared to monomer polymerisation. To form a network structure, both functional groups of the MBAA crosslinker should be incorporated into the network.[32] Once one functional group is incorporated into the polymer, the other has a lower probability of being incorporated owing to the low mobility of the polymers tethered to the existing network.

Surprisingly, mechanoradical polymerisation in the c-DN gels lasted for hours with a continuous monomer supply from the circulating channel. Because polymerisation was triggered by the mechanoradicals generated in the first stretch cycle at a concentration of ~10 μM (Supporting Information), the observed growth of PNaAMPS indicates that some radicals were still alive at 360 min. We conjecture that the growing polymers that are tethered to the network have a very low probability of chain termination reactions owing to suppressed thermal motion, such as the grafting of radicals and a crowding environment. Such long-existing macroradicals are more commonly discussed in glassy or crystalline polymers such as polyethylene and polymethylmethacrylate.[33-37] This unique feature of mechanoradical reactions in DN gels needs to be studied in detail in future work.

Conclusions

We incorporated a channel inside the DN hydrogel that functioned as a monomer perfusion path. Analogous to muscle growth, which is sustained by nutrients from blood vessels, vascular perfusion in the c-DN gel cleared obstacles for replenishing monomers during the self-growing process. Instead of requiring underwater conditions, the c-DN gel can obtain monomers from the circulatory flow of an independently controllable solution supply. Through the diffusion of monomers into the permeable c-DN gels, mechanochemical growth can be readily tuned by changing the monomer concentration flowing through the channel, allowing us to directly control the mechanical growth and trace the corresponding variations in the chemical components. We observed a pronounced difference between the increasing trend of the PNaAMPS content and the mechanical parameters. Using Raman spectroscopy, we detected discrepancies in the kinetics of polymer growth and mechanical strengthening, which may help to better understand the self-growth of DN gels and promote their use in applications such as soft robotics, real-time spectrum monitoring, and mechanochemical reactors.

Experimental section

c-DN hydrogel fabrication

The internal channel of the DN hydrogel was fabricated using sacrificial moulds.[38] A glass capillary tube was used to mould the channel structure during the curing of the PNaAMPS first network. The mould for fixing the capillaries was fabricated using a 3D printer (AGILISTA-3000, Keyence) as shown in Fig. S2. The 0.5 mm capillaries were inserted into the mould and sandwiched between two 10 cm × 10 cm glass plates (Fig. S3). The capillaries were fixed in the middle of the curing chamber. Then, the precursor aqueous solution of the first network containing NaAMPS (1 M), MBAA (2.5 mol% with respect to the monomer), and 2-oxoglutaric acid (1.0 mol% with respect to the monomer) were poured into the mould and irradiated under UV light for 9 h in an Ar atmosphere. The PNaAMPS hydrogel was then laser-cut into rectangular pieces with a capillary in the middle, and immersed in the precursor aqueous solution of the second network gel containing AAm (3 M), MBAA (0.01 mol%), and 2-oxoglutaric acid (0.01 mol%).

After the PNaAMPS gels reached the swelling equilibrium, the channel was almost three times wider in diameter. Consequently, the capillaries can be easily removed. Then, we used high-pressure air to blow away the solutions inside the channel and inserted another capillary tube (1.4 mm) to maintain the channel shape. Finally, the gel was sandwiched between two glass plates and irradiated with UV light for 9 h in an Ar atmosphere to synthesise the second PAAm network. The DN gels were then immersed in a large volume of water to remove unreacted reagents. The channel diameter of the c-DN gel was ~1.6 mm at equilibrium.

Fluorescence observation using LSCM.

A laser scanning confocal microscope (Nikon A1 Rsi and Ti-E, Nikon Co.) was used to observe the in situ mechanoradical polymerisation of NIPAAm. The sample temperature (45 °C) was adjusted using a stage-top incubator (INUBG2H-TIZB, Tokai Hit Co.). We used a Plan Fluor x4 objective lens (NA 0.13, Nikon Co.) and set the excitation laser wavelength to 402.5 nm. For quantification purposes, the fluorescence emission for all measurements was set in the wavelength range of 425–475 nm under the same laser intensity.

Self-growth of c-DN gel supplied by channel flow.

We used the commercial tensile tester (MCT-2150, A&D Co.) inside a glove box to apply a cyclic tensile force trigger on the hydrogel at a crosshead velocity of 100 mm min^{-1} and lifted to a displacement of 105 mm. Then, the crosshead returned to its original state until the next cyclic tensile stretch.

SEM observation before and after self-growth.

To prepare samples for scanning electron microscopy (SEM, JSM-6010LA, JEOL Ltd.), $M_{0.10}C_{0.10}$ and $M_{0.04}C_{0.04}$ gels were collected after the fourth stretch and immersed in a large volume of water to remove unreacted monomers. After reaching a new equilibrium state, the samples were freeze-dried (Advantage XL-70, VirTis freeze-dryer), and the gel surface was coated with gold using an ion-sputtering device (E-1010, Hitachi, Japan).

Raman spectroscopy for detecting constitution change.

Raman spectroscopy (RENISHAW, inVia Reflex) was performed using 532-nm laser as an excitation source, and the incident power was set to 10 mW. The focal spot was adjusted to the channel wall of the c-DN gel. For quantification, a similar area of each sample (middle part of the gauge) was considered for detection. For the c-DN gels subjected to repeated cyclic tensile tests, the $M_{0.10}C_{0.10}$ and $M_{0.04}C_{0.04}$ gels were collected after each stretch. To detect the progress of mechanochemical growth, $M_{0.10}C_{0.10}$ gels grown for various durations (5–360 min) after the first stretch were collected. To quench the mechanoradical polymerisation, the samples were removed from the deoxygenated atmosphere immediately after growth. The gels were then immersed in a large volume of distilled water for one week, during which we repeatedly exchanged the soaking water to remove unreacted monomers before the Raman measurements.

Author Contributions

J. P. G., D. K. and T. N. conceived the idea and supervised the entire project. G. W. and Y. K. conducted experiments. G. W. analysed the data. G. W., N.T. and J. P. G wrote the manuscript. All the authors participated in the discussion.

Conflicts of interest

The authors declare no competing financial interest.

Acknowledgement

This research is supported by the Japan Society for the Promotion of Science (JSPS) KAKENHI (grant nos. JP22H04968, JP22K21342) and by JST, PRESTO grant Number JPMJPR2098. G.W. thanks the MEXT Japan for scholarship during her Ph.D. study.

Notes and references

‡ Image source in Fig. 1a are assets from Freepik.com.

1 P. S. Hwang and D. S. Willoughby, J Strength Cond Res, 2019, **33**, S167-S179.
2 Z. S. Kean and S. L. Craig, Polymer, 2012, **53**, 1035-1048.
3 T. Matsuda, R. Kawakami, R. Namba, T. Nakajima and J. P. Gong, Science, 2019, **363**, 504-508.
4 J. P. Gong, Soft Matter, 2010, **6**, 2583-2590.
5 T. Matsuda, R. Kawakami, T. Nakajima and J. P. Gong, Macromolecules, 2020, **53**, 8787-8795.
6 Z. J. Wang, J. L. Jiang, Q. F. Mu, S. Maeda, T. Nakajima and J. P. Gong, J Am Chem Soc, 2022, **144**, 3154-3161.
7 Q. F. Mu, K. P. Cui, Z. J. Wang, T. Matsuda, W. Cui, H. Kato, S. Namiki, T. Yamazaki, M. Frauenlob, T. Nonoyama, M. Tsuda, S. Tanaka, T. Nakajima and J. P. Gong, Nat Commun, 2022, **13**, 6213.
8 T. Ouchi, B. H. Bowser, T. B. Kouznetsova, X. J. Zheng and S. L. Craig, Mater Horiz, 2023, **10**, 585-593.
9 E. Ducrot, Y. L. Chen, M. Bulters, R. P. Sijbesma and C. Creton, Science, 2014, **344**, 186-189.
10 M. K. Pugsley and R. Tabrizchi, J Pharmacol Tox Met, 2000, **44**, 333-340.
11 A. R. Hamilton, N. R. Sottos and S. R. White, Adv Mater, 2010, **22**, 5159-5163.
12 M. Garg, J. E. Aw, X. Zhang, P. J. Centellas, L. M. Dean, E. M. Lloyd, I. D. Robertson, Y. Q. Liu, M. Yourdkhani, J. S. Moore, P. H. Geubelle and N. R. Sottos, Nat Commun, 2021, **12**, 2836.
13 M. F. Refojo, J Appl Polym Sci, 1965, 9, 3417-3426.
14 K. M. Tarpenning, R. A. Wiswell, S. A. Hawkins and T. J. Marcell, J Sci Med Sport, 2001, **4**, 431-446.
15 J. Crank, The mathematics of diffusion, Clarendon Press, Oxford, Eng, 2d edn., 1975.
16 L. Johansson, C. Elvingson and J. E. Lofroth, Macromolecules, 1991, **24**, 6024-6029.
17 L. Johansson, U. Skantze and J. E. Lofroth, Macromolecules, 1991, **24**, 6019-6023.
18 D. Lin-Vien, N. B. Colthup, W. G. Fateley and J. G. Grasselli, The Handbook of Infrared and Raman Characteristic Frequencies of Organic Molecules, Academic Press, 1991.
19 N. Devi and A. Narzary, Int J Polym Mater, 2012, **61**, 821-833.
20 A. Selvarajan, Proceedings of the Indian Academy of Sciences - Section A, 1966, **64**, 44–50.
21 D. S. Warren and A. J. McQuillan, J Phys Chem B, 2008, **112**, 10535-10543.
22 Y. Sekine and T. Ikeda-Fukazawa, J Chem Phys, 2009, **130**, 034501.
23 D. Ito and H. Itagaki, Eur Polym J, 2018, **99**, 277-283.
24 D. C. Turner and L. Brand, Biochemistry-Us, 1968, **7**, 3381-3390.
25 R. T. M. Jakobs, S. Ma and R. P. Sijbesma, Acs Macro Lett, 2013, **2**, 613-616.
26 S. Ahmed, T. Nakajima, T. Kurokawa, M. A. Haque and J. P. Gong, Polymer, 2014, **55**, 914-923.
27 T. Matsuda, T. Nakajima, Y. Fukuda, W. Hong, T. Sakai, T. Kurokawa, U. Chung and J. P. Gong, Macromolecules, 2016, **49**, 1865-1872.

28 T. Nakajima, Y. Ozaki, R. Namba, K. Ota, Y. Maida, T. Matsuda, T. Kurokawa and J. P. Gong, Acs Macro Lett, 2019, **8**, 1407-1412.
29 G. F. Widhopf and S. Lederman, Aiaa J, 1971, **9**, 309-316.
30 P. Bour, J. Kapitan and V. Baumruk, J Phys Chem A, 2001, **105**, 6362-6368.
31 F. D'Amico, B. Rossi, G. Camisasca, F. Bencivenga, A. Gessini, E. Principi, R. Cucini and C. Masciovecchio, Phys Chem Chem Phys, 2015, **17**, 10987-10992.
32 S. Abrol, M. J. Caulfield, G. G. Qiao and D. H. Solomon, Polymer, 2001, **42**, 5987-5991.
33 S. I. Ohnishi and I. Nitta, J Polym Sci, 1959, 38, 451-458.
34 S. Nara, S. Shimada, H. Kashiwabara and J. Sohma, J Polym Sci A2, 1968, **6**, 1435-1449.
35 S. Shimada and Kashiwab.H, Polym J, 1974, **6**, 448-450.
36 S. Shimada, Prog Polym Sci, 1992, **17**, 1045-1106.
37 P. J. Butiagin, Pure and Applied Chemistry, 1972, **30**, 57–76.
38 J. S. Miller, K. R. Stevens, M. T. Yang, B. M. Baker, D. H. T. Nguyen, D. M. Cohen, E. Toro, A. A. Chen, P. A. Galie, X. Yu, R. Chaturvedi, S. N. Bhatia and C. S. Chen, Nat Mater, 2012, **11**, 768-774.